EUROPEAN ORGANIZATION FOR NUCLEAR RESEARCH

CERN–PPE/95–158
2 November 1995

MEASUREMENT OF α_s FROM $b\bar{b}$ PRODUCTION AT THE CERN $p\bar{p}$ COLLIDER

The UA1 Collaboration

Aachen[1] - Amsterdam (NIKHEF)[2] - Birmingham[3] - CERN[4] - Helsinki[5] - Kiel[6] - Imperial College, London[7] - Queen Mary and Westfield College, London[8] - MIT[9] - Rutherford Appleton Lab[10] - Saclay[11] - UCLA[12] - Vienna[13]

C. Albajar[4,a], K. Ankoviak[12], S. Bartha[6], G. Bauer[9], A. Bezaguet[4], A. Böhrer[1,b], K. Bos[2], C. Buchanan[12], B. Buschbeck[13], H. Castilla-Valdez[12], P. Cennini[4], S. Cittolin[4], E. Clayton[7], D. Cline[12], J.A. Caughlan[10], D. Dau[6], C. Daum[2], M. Della Negra[4], M. Demoulin[4], D. Denegri[11], H. Dibon[13], J. Dorenbosch[2], J.D. Dowell[3], K. Eggert[4], E. Eisenhandler[8], N. Ellis[3,4], H. Evans[12,c], H. Faissner[1], I.F. Fensome[3], L. Fortson[12], J. Garvey[3], A. Geiser[1,4], A. Givernaud[4], A. Gonidec[4], B. Gonzalez[12*], J. Gronberg[12], D.J. Holthuizen[2], W. Jank[4], G. Jorat[4], P.I.P. Kalmus[8], V. Karimäki[5], I. Kenyon[3], R. Kinnunen[5], M. Krammer[13], S. Lammel[1,12], M.P.J. Landon[8], Y. Lemoigne[11], S. Levegrün[6], P. Lipa[13], C. Markou[7], M. Markytan[13], G. Maurin[4], S. McMahon[7], J.P. Merlo[11], T. Meyer[4], T. Moers[1], M. Mohammadi[12,d], A. Morsch[6,4], A. Moulin[1,e], A. Norton[4], S. Otwinowski[12], G. Pancheri[9], E. Pietarinen[5], M. Pimiä[5], A. Placci[4], J.P. Porte[4], R. Priem[1], R. Prosi[6], E. Radermacher[4], M. Rauschkolb[6],H. Reithler[1], J.P. Revol[9,4], D. Robinson[8,f], C. Rubbia[4], D. Samyn[4], D. Schinzel[4], R. Schleichert[1,g], M. Schröder[2],C. Seez[7], T.P. Shah[10], P. Sphicas[9], D. Stork[12], K. Sumorok[9], F. Szoncso[13], C.H. Tan[9], A. Taurok[13], L. Taylor[7], S. Tether[9], H. Teykal[1], G. Thompson[8], H. Tuchscherer[1,h], J. Tuominiemi[5], W. van de Guchte[2], A. van Dijk[2], M. Vargas[12], T.S. Virdee[7], W. von Schlippe[8], V. Vuillemin[4], K. Wacker[1,i], H. Wagner[1], G. Walzel[13], C.-E. Wulz[13], and P. Zotto[4,j]

(Submitted to Physics Letters B)

[1] III. Physikalisches Institut A, Physikzentrum RWTH, Arnold Sommerfeld Straße, D-52074 Aachen, Germany
[2] NIKHEF-H, Kruislaan 409, Postbus 41882, NL-1009 DB Amsterdam, The Netherlands
[3] Department of Physics, University of Birmingham, P.O. Box 363, Birmingham B15 2TT, UK
[4] CERN, CH-1211 Geneva 23, Switzerland
[5] Laboratory of HEP, Department of Physics, or Research Institute for HEP (SEFT), University of Helsinki, P.O. Box 9, Siltavuorenpenger 20C, SF-00014 Helsinki, Finland
[6] Institut für Reine und Angewandte Kernphysik, Christian Albrechts Universität, Olshausenstraße 40-60, D-24118 Kiel, Germany
[7] Blackett Laboratory, Imperial College, Prince Consort Road, London SW7 2BZ, UK
[8] Department of Physics, Queen Mary and Westfield College, Mile End Road, London E1 4NS, UK
[9] Laboratory for Nuclear Science, MIT, 77 Massachusetts Avenue, Cambridge, MA 02139, USA
[10] Rutherford Appleton Laboratory, Chilton, Didcot, Oxon OX11 0QX, UK
[11] DPHPE/SEPh, CEN Saclay, B.P. 2, F-91190 Gif-sur-Yvette, France
[12] University of California at Los Angeles, 405 Hilgard Avenue, Los Angeles, CA 90024, USA
[13] Institut für Hochenergiephysik, Österreichische Akademie der Wissenschaften, Nikolsdorfergasse 18, A-1050 Vienna, Austria

[a] present address: Facultad de Ciencias, Universidad Autonoma, Cantoblanco, 28049 Madrid, Spain
[b] present address: Universität Siegen, Germany
[c] present address: Enrico Fermi Institute, University of Chicago, Chicago, IL 60637, USA
[d] present address: Department of Physics, SUNY, Stony Brook, NY 11794, USA
[e] present address: American Management Systems, Essen, Germany
[f] present address: Cambridge University, Cambridge, UK
[g] present address: Forschungszentrum Jülich, Germany
[h] present address: University of Alabama, Tuscaloosa, USA
[i] present address: Universität Dortmund, Germany
[j] present address: Dipartimento di Fisica del Politecnico di Milano, Milano, Italy

[*] deceased

Abstract

The UA1 Collaboration has recently improved its measurement of the beauty production cross-section by including explicit measurements of $b\bar{b}$ correlations. Using these data we have determined the strong coupling constant α_s. The comparison of the measured cross-section for 2-body final states with $O(\alpha_s^3)$ QCD predictions yields a measurement of $\alpha_s(20\ \text{GeV}) = 0.145^{+0.012}_{-0.010\,\text{exp}}{}^{+0.013}_{-0.016\,\text{th}}$, corresponding to $\alpha_s(M_Z) = 0.113^{+0.007}_{-0.006\,\text{exp}}{}^{+0.008}_{-0.009\,\text{th}}$. This is the first theoretically well-defined measurement of α_s from a purely hadronic production process. Evaluating α_s from cross-sections at different Q^2-values we find that the running of α_s is needed for internal consistency of the UA1 data.

1 INTRODUCTION

Despite the fact that the theory of Quantum Chromodynamics (QCD) yields adequate qualitative and quantitative predictions of high E_T jet, heavy-flavour, and single-photon production at hadron colliders, quantitative measurements of the parameters of this theory, e.g. the strong coupling constant α_s, have been obtained mainly from QCD corrections to dominantly electroweak processes (e^+e^--collisions, deep inelastic scattering, $p\bar{p} \rightarrow W + jet$) [1].

The lack of measurements of comparable precision from purely hadronic interactions had several reasons:

- The poorly defined initial state involving the convolution of two hadronic structure functions.
- Final-state fragmentation of the primary quarks and gluons resulting from the hard scattering process, and the difficulty of their separation from the fragmentation products of the spectator partons (underlying event).
- The complexity of the theoretical QCD predictions, especially for the calculation of contributions beyond leading order.

Early measurements of α_s from jet production at the CERN $p\bar{p}$ collider [2] were therefore only obtained up to a theoretically problematic K-factor. Here we exploit the considerable progress which has been made in all of these areas to present the first theoretically well-defined measurement of α_s from a purely hadronic production process. The beauty production processes considered in this analysis offer some particular advantages over other hadronic processes:

- A fully differential next-to-leading order ($O(\alpha_s^3)$) QCD prediction is available [3].
- The hard fragmentation of the rather massive b quarks considerably reduces the uncertainty associated with jet fragmentation.
- The structure functions in the kinematic range used for this analysis are relatively well constrained.

We use these properties to extract a measurement of the strong coupling constant from the measured absolute beauty production cross-sections at the CERN $p\bar{p}$ collider. The results presented in this paper are the final update of an earlier preliminary result [4].

2 CROSS-SECTIONS FOR BEAUTY PRODUCTION

Cross-sections for beauty production at the CERN $p\bar{p}$ collider have been measured from a variety of $b\bar{b}$ production and decay processes [5, 6, 7]. A representative fraction of these b quarks is detected in UA1 through their semileptonic decays, yielding high transverse momentum muons which are nonisolated, i.e. accompanied by hadrons from fragmentation and decay of the parent parton. Transverse momentum (p_T) is measured with respect to the beam axis. The UA1 detector is described elsewhere [8]. Muons are identified by their ability to penetrate more than 8 interaction lengths of material, leaving tracks in the outer muon chambers. Good efficiency is obtained for $p_T^\mu > 3$ GeV/c, and muon pseudorapidity acceptance extends up to $|\eta| = 2.3$ for dimuon events.

The strong correlation between the momenta of the original quark and the resulting decay muons allows a determination of the b quark production cross-section from the measured muons alone, avoiding a complicated jet algorithm. The uncertainty due to the underlying event is therefore almost completely eliminated.

The hard fragmention of b quarks is well measured at e^+e^- colliders and the resulting error on our measured cross-sections is small (6–12%). Branching ratios and decay kinematics are also known from e^+e^- studies, and the considerable momentum smearing due to the semileptonic decay of B-hadrons is partially accounted for by measuring integrated rather than differential cross-sections as a function of p_T.

Finally, the study of dimuon events where the two muons originate from different quarks of a $b\bar{b}$ pair allows the measurement of $b\bar{b}$ correlations [7], and therefore the direct measurement of higher order contributions. Since the separation of lowest order and higher order contributions is an important ingredient of the α_s determination, the criterion used for this separation will now be considered in some detail.

While the leading order $O(\alpha_s^2)$ contributions produce back-to-back $b\bar{b}$ configurations ($\Delta\phi = 180°$, where $\Delta\phi$ is the azimuthal angle difference between the two quarks), higher order processes can yield any $\Delta\phi$ value. For an approximate separation of the lowest and higher order contributions we introduce the concept of *(quasi-)2-body* and *3-body* final states (Fig. 1) which we *define* as

$$\begin{aligned} \text{2-body final state} &\equiv \Delta\phi(b\bar{b}) > 150° \\ \text{3-body final state} &\equiv \Delta\phi(b\bar{b}) < 150° \ . \end{aligned} \tag{1}$$

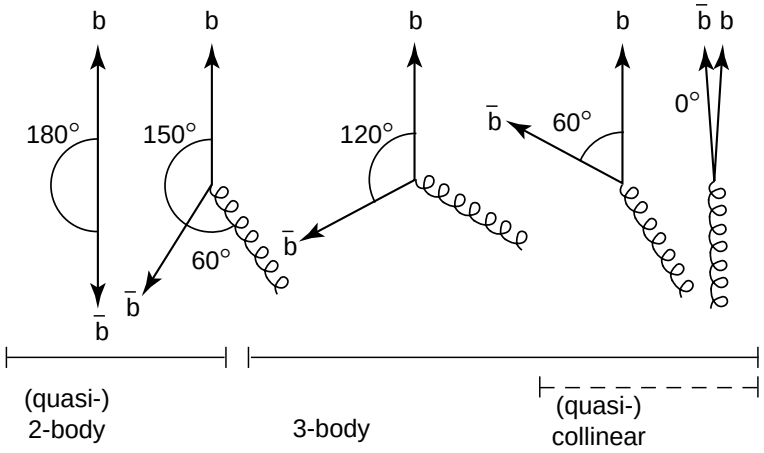

Figure 1: Some typical event configurations in the transverse plane.

This phenomenological definition has several advantages:

- It is theoretically and experimentally well-defined.
- To lowest order, $\sigma_{LO} \equiv \sigma_{\text{2-body}}$, and the $O(\alpha_s^3)$ corrections to $\sigma_{\text{2-body}}$ are *small* and *stable* (Section 4).
- Only the *direction* of the *heavy quark* momenta in the laboratory system is needed. This is much easier to measure than the full momentum. Identification of other final-state partons, e.g. a gluon, is not explicitly required.
- The choice of 150° for the separation is half way between the true 2-body configuration (back-to-back) and the typical 3-body 'Mercedes' configuration (Fig. 1). This choice is compatible with the UA1 b quark angular resolution ($\sim$ 10–15°) [9].

The expected contributions of 2-body (3-body) final states to $b\bar{b}$ production at the CERN collider are about 60% (40%) respectively. A corresponding breakdown of the measured inclusive cross-sections into cross-sections for b quarks from 2-body and 3-body

final states is shown in Fig. 2 (see Refs. [7, 9] for the treatment of collinear gluons in the b quark definition).

The reasons for the large expected next-to-leading order contributions are explained in Refs. [7, 10, 11]. In short, they are due to enhanced gluon splitting diagrams giving rise to 3-body topologies. In contrast, partial calculations of even higher orders show that the next-to-next-to-leading contributions yielding 4-body topologies are expected to be small [10].

Noting that, to the respective leading order, the measured 2-body and 3-body b quark cross sections are proportional to specific powers of α_s:

$$\sigma_{\text{2-body}} \sim \alpha_s^2 \tag{2}$$

$$\sigma_{\text{3-body}} \sim \alpha_s^3 \tag{3}$$

we can measure α_s from these cross-sections by fitting the theoretical QCD parameters.

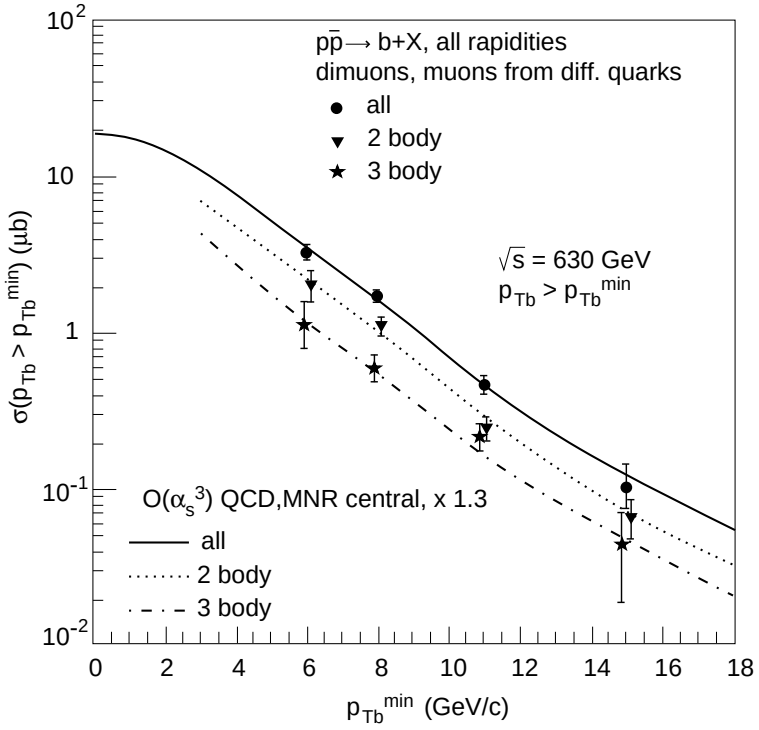

Figure 2: The single b quark cross-section from dimuon events for all rapidities and $p_{Tb} > p_{Tb}^{\min}$ in p$\bar{\text{p}}$ collisions at $\sqrt{s} = 630$ GeV [7]. The inclusive cross-section is separated into cross-sections for b quarks from 2-body and 3-body final states. Only the p_T-dependent errors are shown. A global error of 28% has to be added to all data points. Also shown is the central $O(\alpha_s^3)$ prediction from Ref. [3], normalized to the data using a global factor which is well within the theoretical error.

3 CHOICE OF THE STRUCTURE FUNCTIONS

To measure α_s or, equivalently, the QCD scale parameter Λ from the absolute normalization of the measured b production cross-sections, a good knowledge of the contributing structure functions (parton density functions) is essential. Next-to-leading order structure functions are needed for consistency with the $O(\alpha_s^3)$ QCD calculation. Since the

cross-sections in the $p_T^{\min}$ range 6–15 GeV/c are dominated by gluon–gluon initial states we will focus on the gluon density functions in the following.

The uncertainties due to the choice of the structure functions can be broken down into two basic categories [12]:

- Errors due to lack of experimental knowledge of the input gluon distribution, especially at small x, which are correlated with errors on Λ.
- Errors due to uncertainties on the Λ value used for the structure function evolution.

As a representative up-to-date structure function, we have chosen the set MRSD$-'$ [13], which is compatible with recent HERA data [14]. For a conservative estimate of the error due to the structure function choice, we use the 'classic' next-to-leading order sets DFLM 160,260,360 [15] and MRS 1,2,3 [16]. Figure 3 shows that these structure functions are a representative sample out of all possible choices [17], for both shape and normalization. Also, they are derived from deep inelastic scattering (DIS) only and are therefore independent of collider data.

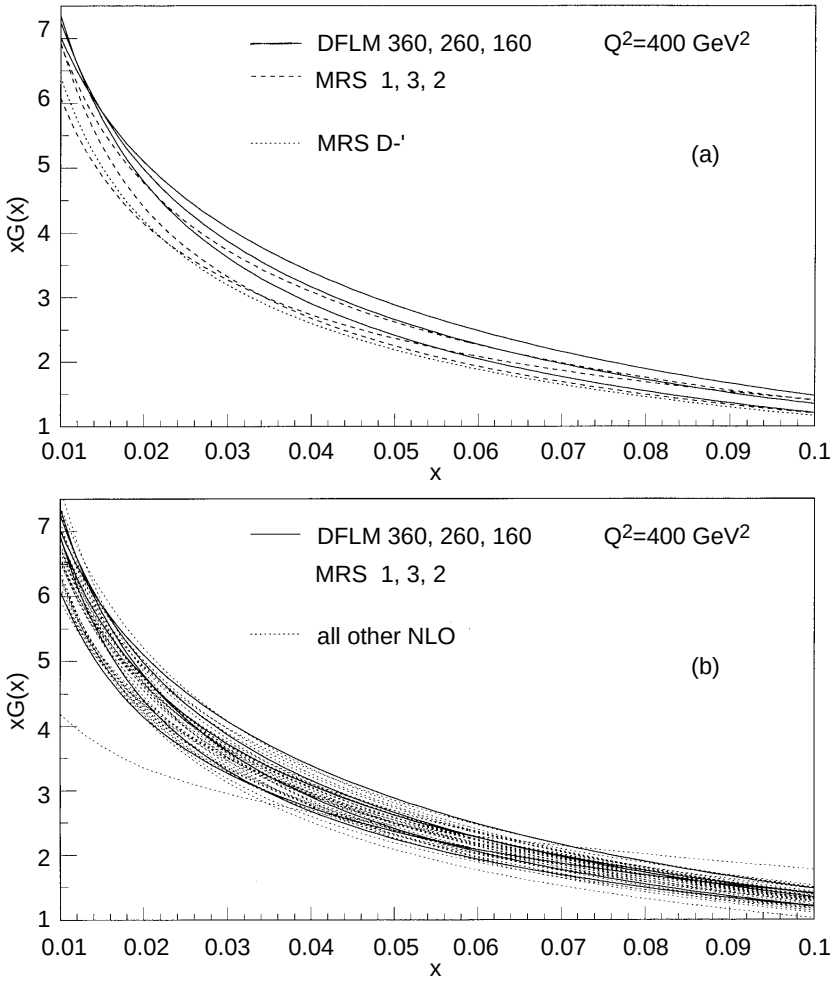

Figure 3: The gluon density functions used in this analysis. Only the x range relevant for heavy-flavour production at the CERN collider is shown. For each line style, the labels are ordered from top to bottom at $x = 0.03$. (a) The structure functions used in this analysis.
(b) The structure functions from (a) compared to all other available next-to-leading order (NLO) structure functions from Ref. [17]. The curve deviating from all others corresponds to an unphysical 'valence gluon' density function.

From a study using the special sets MRS B0 [12] we find that the gluon density functions at $Q = 20$ GeV are determined mainly by the choice of the input density functions at DIS energies, and only to a lesser extent by the variation of Λ used for the Q^2 evolution. We also find that the predicted cross-section is about 5 times more sensitive to a variation of the external Λ value explicitly appearing in the cross-section calculation than to the internal value used to generate the tabulated structure functions. This is to be expected from the analysis of the renormalization group equation for the cross-section. The structure functions (with their associated fixed Λ value) and the Λ used for the external α_s calculation are therefore varied independently. Since the fitted external Λ values will turn out to be compatible with the internal ones to within 1 σ in each case, the small error due to the inconsistency of the two Λ values will be assumed to be contained in the band of different structure functions used.

4 CHOICE OF THE RENORMALIZATION AND FACTORIZATION SCALES

For finite-order QCD calculations, the predicted cross-sections depend on the chosen renormalization scheme, and on the reference scale chosen for the expansion of the parton–parton cross-sections (renormalization scale) and structure functions (factorization scale) in powers of α_s. The so-called $\overline{MS}$ minimal subtraction scheme [18] is adopted in the calculations of Mangano, Nason, and Ridolfi (MNR) [3] relevant for this analysis, and the standard next-to-leading order expression [19] is used for the parametrization of $\alpha_s(Q^2)$ in terms of $\Lambda_{\overline{MS}}$.

It is common practice to estimate the theoretical error due to uncalculated higher order corrections by varying these scales within physically sensible ranges. By separately varying the renormalization and factorization scales for the $b\bar{b}$ calculations in the relevant kinematic range, we find a positive correlation for the cross-section dependence on these two scales, and dominance of the renormalization scale variation. It is therefore safe to define only a single scale $\mu = \mu_{\rm ren} = \mu_{\rm fact}$, and to vary only this single scale. We adopt this simplifying procedure for all analyses described in this paper.

An example for the dependence of the QCD prediction for the 2-body and 3-body cross-sections on the choice of the renormalization/factorization scale μ is shown in Fig. 4. The $O(\alpha_s^3)$ corrections make the predicted 2-body cross-section fairly stable against scale variations, as expected for a next-to-leading order calculation. In contrast, the 3-body cross-section shows a very strong μ dependence, since it is effectively calculated to leading order only. $O(\alpha_s^4)$ calculations which would stabilize this behaviour are not currently available. For the inclusive cross-section, the large 3-body contribution also imposes a fairly strong μ-scale dependence, suggesting a large theoretical error.

We will therefore use only the measured 2-body cross-sections for our main α_s determination. The inclusive and 3-body cross-sections will however yield an important cross-check of our result, and indicate that the result is stable against variations of the 2-body/3-body definition.

To estimate reasonable values for the choice of the renormalization/factorization scale, we use three different criteria:

- The 'natural' scale of the process, $\mu_0 = \sqrt{m_b^2 + p_T^2}$, introduced in [10]. This scale will also be used as a reference scale.

- The scale which leaves the leading order calculation unchanged when going to next-to-leading order, without adding new topologies. This corresponds to the requirement $\sigma_{\text{2-body}}(\mu) \simeq \sigma_{\text{LO}}(\mu)$ and suggests $\mu \simeq \mu_0/2$ (Fig. 4).
- The scale at which the cross-section is stable against small variations of μ ($d\sigma/d\mu = 0$). Applying it to the 2-body cross-section yields $\mu \simeq \mu_0/4$ (Fig. 4).

Considering that e.g. the measurement of jet shapes at CDF [20] favours a scale range $E_T/4 < \mu < E_T$, the values obtained look rather reasonable. We will hence use the range $\mu_0/4 < \mu < \mu_0$ for our α_s determination, corresponding to a variation in μ^2 of a factor 16. This choice will further be validated by an independent fit to the data (Section 5).

To cope with uncertainties in the shape of the QCD prediction we introduce a more general parametrization of the reference scale of the form

$$\mu_0 = \sqrt{(k \times m_b)^2 + p_T^2}, \quad k = 1.0^{+0.50}_{-0.33} \,. \tag{4}$$

The additional k parameter was introduced in an earlier analysis [7] for the extraction of the total $b\bar{b}$ cross-section from the data and mainly affects the shape of the cross-section prediction at low p_T. It allows the evaluation of the sensitivity to different linear combinations of p_T and m_b in the choice of μ_0, and turns out to be only of minor importance for the α_s determination.

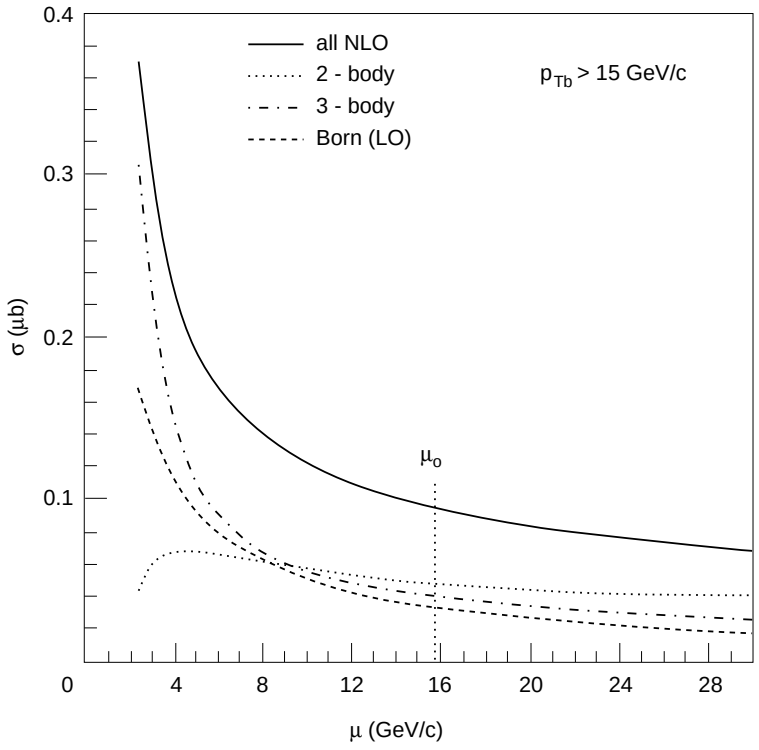

Figure 4: Scale dependence of the single b quark cross-section for $p_{Tb} > 15$ GeV/c, evaluated at leading (LO) and next-to-leading (NLO) order using the calculations from Ref. [10, 3]. The NLO cross-section is separated into cross-sections for b quarks from 2-body and 3-body final states.

5 THE MEASUREMENT OF α_s

For our basic α_s measurement we use the four measured 2-body cross-sections of Fig. 2, yielding a combined experimental normalization error of 29%. Unfolding the structure function dependence, a fit of the $O(\alpha_s^3)$ QCD prediction to these data (shape and normalization) yields a direct measurement of α_s *squared*.

In summary, the theoretical parameters varied in the fit are:

- The QCD scale parameter $\Lambda^5_{\overline{MS}}$ (five active flavours) yielding the value of α_s.
- The renormalization/factorization scale μ as discussed in Section 4. The fit is performed with the scale *fixed* to $\mu = \mu_0/4$, $\mu_0/2$, and μ_0, respectively, taking the result for $\mu = \mu_0/2$ as the central value and the variation as the error. The shape parameter k (see above) is constrained to $2/3 < k < 3/2$.
- The b quark mass m_b, constrained to the range 4.5 GeV/$c^2 < m_b <$ 5 GeV/c^2. The variation of m_b is strongly correlated with the variation of k, but also affects phase space calculations and energy thresholds.
- The structure functions for the gluon and quark contents of the incoming protons and antiprotons as discussed in Section 3. The set MRSD$-'$ [13] is used to obtain the central value. The fit is also performed separately for each of the DFLM and MRS structure functions discussed above, and the spread of the results is taken to be the error due to this source.

All these quantities are fitted simultaneously to the four measured 2-body cross-sections of Fig. 2 using the prediction of the $O(\alpha_s^3)$ QCD calculation [3] and accounting for correlations. The uncertainties on the fragmentation and decay of the b quarks are contained in the experimental error associated to the measured b quark cross-sections. From the results listed in Table 1 we obtain a measurement of the QCD scale parameter for five active flavours in the $\overline{MS}$ scheme

$$\Lambda^5_{\overline{MS}} = 169 \, {}^{+87}_{-55}{}_{\rm exp} \, {}^{+18}_{-21}{}_{k,m_b} \, {}^{+66}_{-66}{}_{\mu} \, {}^{+46}_{-55}{}_{\rm str.f.} \ {\rm MeV} \tag{5}$$

where the first error is dominated by the experimental normalization error, and the second arises from the strongly correlated parameters k and m_b. The third error corresponds to the variation of the renormalization/factorization scale in the range $\mu_0/4 < \mu < \mu_0$, and the last error reflects the effect of the variation of the structure functions. Using the next-to-leading order formulas from [19] we obtain

$$\alpha_s(20 \text{ GeV}) = 0.145 \, {}^{+0.012}_{-0.010}{}_{\rm exp} \pm 0.003_{k,m_b} \, {}^{+0.010}_{-0.012}{}_{\mu} \, {}^{+0.007}_{-0.010}{}_{\rm str.f.} \tag{6}$$

The chosen scale of (20 GeV)^2 reflects the typical Q^2 of the $b\bar{b}$ data events. Combining the theoretical errors we obtain our final result

$$\alpha_s(20 \text{ GeV}) = 0.145 \, {}^{+0.012}_{-0.010}{}_{\rm exp} \, {}^{+0.013}_{-0.016}{}_{\rm th} \tag{7}$$

corresponding to $\alpha_s(M_Z) = 0.113 \, {}^{+0.007}_{-0.006}{}_{\rm exp} \, {}^{+0.008}_{-0.009}{}_{\rm th}$.

As a cross-check for the self-consistency of our α_s determination we also perform a combined fit of the 2-body *and* 3-body cross-sections (Table 2). The strong μ dependence of the 3-body cross-section allows an empirical fit of the preferred renormalization/factorization scale as a *free* parameter. Although theoretically less meaningful the

obtained result, $\alpha_s(M_Z) = 0.113^{+0.009}_{-0.013}$, is fully consistent with the result of the 2-body fit. Furthermore, the fitted preferred scale

$$\mu/\mu_0 = 0.5 \pm 0.2_{\mathrm{exp},k,m_b,\Lambda} \; {}^{+0.2}_{-0.1}{}_{\mathrm{str.f.}} \tag{8}$$

agrees with the range derived from independent theoretical arguments.

We consider this to be an important check of self-consistency. Furthermore the fit of the full (i.e. 2-body + 3-body) cross-section is partially equivalent to a '2-body' fit with the angular threshold for the 2-body definition lowered from 150^0 to 0^0. The fact that the result for α_s remains almost unchanged for this extreme case also suggests the stability of the result against smaller variations of the 2-body/3-body angular threshold.

Table 1: Results of the $\Lambda^5_{\overline{MS}}$ fit for different fixed scales μ/μ_0 (columns) and various sets of structure functions (rows) using the 2-body cross-sections only. The errors quoted in the column for $\mu/\mu_0 = 0.5$ include the errors due to all other parameters (k,m_b and experimental), and are dominated by the experimental error.

Structure function	$\Lambda^5_{\overline{MS}}$ MeV for μ/μ_0 = 0.5	0.25	1.0
MRSD$-'$	169^{+89}_{-59}	103	235
DFLM 160	104^{+52}_{-32}	71	188
DFLM 260	110^{+52}_{-32}	78	201
DFLM 360	130^{+91}_{-39}	91	227
MRS 1	117^{+117}_{-46}	65	234
MRS 2	110^{+234}_{-46}	65	273
MRS 3	214^{+260}_{-110}	91	344

Table 2: Results of the $\Lambda^5_{\overline{MS}}$ fit for 2-body and 3-body cross-sections for different sets of structure functions. The errors on $\Lambda^5_{\overline{MS}}$ include the error due to the free variation of μ, in addition to the errors mentioned in Table 1.

Structure function	$\Lambda^5_{\overline{MS}}$ MeV μ/μ_0 fitted	μ/μ_0	χ^2
MRSD$-'$	173^{+92}_{-74}	$0.46^{+0.24}_{-0.13}$	6.3/6
DFLM 160	78^{+71}_{-26}	$0.4^{+0.15}_{-0.1}$	4.3/6
DFLM 260	84^{+71}_{-26}	$0.4^{+0.15}_{-0.1}$	4.5/6
DFLM 360	110^{+84}_{-39}	$0.45^{+0.15}_{-0.15}$	5.0/6
MRS 1	117^{+130}_{-58}	$0.5^{+0.3}_{-0.15}$	6.2/6
MRS 2	208^{+143}_{-117}	$0.7^{+0.25}_{-0.25}$	8.7/6
MRS 3	221^{+156}_{-130}	$0.65^{+0.2}_{-0.25}$	6.2/6

6 THE RUNNING OF α_s

The *running* of α_s, i.e. the shrinking of its value with increasing Q^2, is one of the main predictions of the theory of QCD. This prediction can be tested by comparing α_s measurements obtained at different Q values. However, such a comparison usually involves the combination of very distinct data sets (e.g. tau-decay vs. Z-decay at LEP [1]) since most experiments only yield α_s measurements at single specific Q-values or corresponding narrow ranges.

Here, we study the running of α_s from the UA1 b production data *alone*, fully exploiting the large measured b quark p_T range. To get a large enough lever arm we include all inclusive b cross-section measurements from single muon events [6] extending up to $p_T^{\min} = 48$ GeV/c. Furthermore we need separate measurements of α_s for each $p_T^{\min}$ value.

To investigate the running of α_s, we use the leading order formula for the α_s evolution

$$\alpha_s(Q) = \frac{\alpha_s(Q_0)}{1 + b_f \alpha_s(Q_0) \log(Q^2/Q_0^2)} \tag{9}$$

with $b_f = \frac{11N_c - 2N_f}{12\pi}$, where N_c is the number of colours and N_f the number of flavours contributing to the QCD evolution. Instead of fixing b_f to its standard QCD value of $b_{f_{QCD}} = 0.61$ (for $N_c = 3$ and $N_f = 5$), we leave this parameter *free* to be fitted from the data, together with the value of $\alpha_s(Q_0)$ choosing $Q_0 = 20$ GeV for the (arbitrary) reference scale.

Since for this study we are only interested in the shape parameter b_f and since the absolute value of $\alpha_s(20\ \text{GeV})$ has already been determined earlier, the parameter $\alpha_s(Q_0)$ will be used only for the normalization to the data without a detailed consideration of its experimental and theoretical error.

Some new problems arise from this approach:

- Since it is not possible to determine the 2-body and 3-body fractions for the single muon measurements, the *inclusive* cross-sections have to be used for this study. Fortunately, the *shape* of the resulting α_s evolution turns out to remain almost unaffected by the strong μ-dependence of this cross-section.
- An appropriate representative Q-value has to be chosen for the α_s determination from each data point. We choose to use a value corresponding to the minimum Q-value of the central hard scatter, $Q = 2 \times \sqrt{m_b^2 + p_{Tb}^{\min\ 2}}$. A different choice would move all data points according to Eq. (9) with $b_f = b_{f_{QCD}}$. Since the result for b_f will turn out to be consistent with $b_{f_{QCD}}$, it does not critically depend upon this choice.
- Since we are only interested in the shape parameter b_f we use the p_T-dependent errors only, where available [7]. In the cases where several measurements exist for the same $p_T^{\min}$ value we combine these measurements taking into account their correlations. However, we choose to ignore the residual correlations between the data points at different $p_T^{\min}$ values. This is a conservative approach for the determination of the shape of the distribution.
- Since a single measurement does not yield enough degrees of freedom to perform a fit, we fix all other theoretical parameters to their central values and simply calculate the value of α_s needed to normalize the $O(\alpha_s^3)$ QCD prediction to the central value of each data point. The experimental error for each point is obtained by repeating the calculation for the 1 σ upper and lower value of the cross-section,

and the theoretical error by a corresponding variation of each of the theoretical parameters involved.

An example of the result of this procedure is shown in Fig. 5.

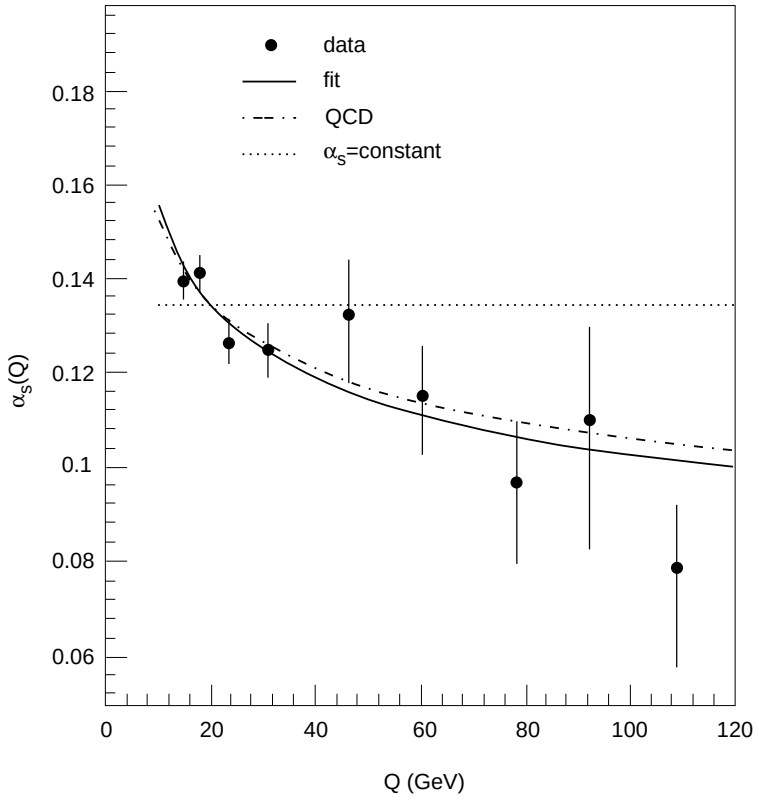

Figure 5: The running of α_s from UA1 data. Shown are the results for α_s as a function of the effective scale Q obtained from each $p_T^{\min}$ bin using the DFLM 260 structure functions, $\mu = 0.5\ \mu_0$ with $\mu_0 = \sqrt{m_b^2 + p_{Tb}^{\min\ 2}}$ $(k = 1)$, and $m_b = 4.75$ GeV/c^2 fixed. Also shown are curves obtained from a fit of the running parameter b_f (continuous line, see text for details), a 'best fit' for the hypothesis of constant α_s (dotted line) and the standard QCD prediction for $\Lambda^5_{\overline{MS}} = 130$ MeV (dash-dotted line), the other theoretical parameters being fixed as quoted above.

For this example it is clear that the fitted slope, $b_f = 0.74 \pm 0.16_{\rm exp}$, is in good agreement with the QCD prediction, while the hypothesis of constant α_s $(b_f = 0)$ is considerably disfavoured. The value of $\alpha_s(Q_0) = 0.136$ obtained from the normalization is consistent with the α_s values measured earlier. Varying all theoretical parameters as indicated in Table 3 and taking the average of the quoted structure functions[1)] yields the final result

$$b_f = \frac{11N_c - 2N_f}{12\pi} = 0.79 \pm 0.16_{\rm exp} \pm 0.19_{\rm th}\ . \qquad (10)$$

This result is in good agreement with the QCD expectation $b_f = 0.61$ for 3 colours and 5 flavours, and disfavours a constant α_s by about 3 standard deviations.

A caveat has to be applied to the quantitative interpretation of this result because the running of α_s has already been used for the Q^2 evolution of the structure functions

[1)] Only DFLM 160 and 360, and MRS 1 and 3 have been used for this evaluation. MRS 2 has been excluded because it is somewhat disfavoured by the α_s analysis (Table 2) due to its extreme shape. It is also disfavoured by other data ([10] and references therein). In order not to give too much weight to the DFLM sets, the intermediate DFLM 260 set has also been omitted from the average.

involved. However, the use of a constant α_s value for this evolution would tend to *increase* the measured slope parameter b_f, and hence increase the inconsistency with the value $b_f = 0$. We therefore conclude that the running of α_s is needed for the internal consistency of the measured UA1 b cross-sections in the framework of QCD.

Table 3: Theoretical error on b_f (see text). The different contributions arising from individual sources are listed. In addition to the standard sources, an error due to the uncertainties on the b quark definition (gluon resummation in cone of $\Delta R < 1$) for large $p_{Tb}^{\min}$ is also included.

Source	Range	Absolute error
Structure functions	DFLM 160,360, MRS 1,3	0.13
$A = \mu/\mu_0$	$0.25 < A < 1$	0.08
k (shape of μ_0)	$2/3 < k < 3/2$	0.07
m_b	$4.5 < m_b < 5.0$ GeV/c^2	0.05
b quark definition	Uncertainty at large $p_{Tb}^{\min}$ [9]	0.06
Combined		0.19

7 CONCLUSIONS

We use our most recent measurements of the beauty production cross-section and $b\bar{b}$-correlations [7] to extract a measurement of the strong coupling constant α_s. The comparison of the measured cross-section for 2-body final states with $O(\alpha_s^3)$ QCD predictions yields

$$\alpha_s(20 \text{ GeV}) = 0.145 \, {}^{+0.012}_{-0.010\,\text{exp}} \, {}^{+0.013}_{-0.016\,\text{th}} \tag{11}$$

corresponding to $\alpha_s(M_Z) = 0.113 \, {}^{+0.007}_{-0.006\,\text{exp}} \, {}^{+0.008}_{-0.009\,\text{th}}$.

Extending the study to previous measurements [6] covering the full accessible Q^2 range, we conclude that the running of α_s is needed for internal consistency of the data in the framework of QCD, using UA1 data only.

Acknowledgements

We are greatly indebted to the authors of Refs. [3] and [10] and in particular to P. Nason for providing us with the programs for the $O(\alpha_s^3)$ QCD calculations and instructing us how to use them.

We are thankful to the management and staff of CERN and of all participating institutes for their vigorous support of the experiment. The following funding agencies have contributed to this programme:

Fonds zur Förderung der Wissenschaftlichen Forschung, Austria; Valtion luonnontieteellinen toimikunta, Suomen Akatemia, Finland; Institut National de Physique Nucléaire et de Physique des Particules and Institut de Recherche Fondamentale (CEA), France; Bundesministerium für Forschung und Technologie, Germany; Istituto Nationale di Fisica Nucleare, Italy; Science and Engineering Research Council, United Kingdom; Stichting Voor Fundamenteel Onderzoek der Materie, The Netherlands; Centro de Investigaciones Energetica, Medioambientales y Tecnologicas (CIEMAT), Spain; Department of Energy, USA.

Thanks are also due to the following people who have worked with the collaboration in the preparations for and data collection on the runs described here: L. Baumard, F. Bernasconi, D. Brozzi, V. Cecconi, L. Dumps and G. Fetchenhauer.

References

[1] see e.g. QCD review by the Particle Data Group, Phys. Rev. **D50** (1994) 1297.

[2] UA1 collaboration, G. Arnison et al., Phys. Lett. **B158** (1985) 494;
UA2 collaboration, J.A. Appel et al., Z. Phys. **C30** (1986) 341.

[3] M.L. Mangano, P. Nason and G. Ridolfi, Nucl. Phys. **B373** (1992) 295.

[4] A. Geiser (UA1 collaboration), proceedings of the XXVIIth Rencontre de Moriond, Perturbative QCD and Hadronic Interactions, Les Arcs, France, 22–28 March 1992, ed. by Tran Thanh Van (Editions Frontières, Gif-sur-Yvette,1992) p. 159, and PITHA 92/19 (1992).

[5] UA1 collaboration, C. Albajar et al., Phys. Lett. **B213** (1988) 405.

[6] UA1 collaboration, C. Albajar et al., Phys. Lett. **B256** (1991) 121.

[7] UA1 collaboration, C. Albajar et al., Z. Phys. **C61** (1994) 41.

[8] UA1 collaboration, C. Albajar et al., Z. Phys. **C48** (1990) 1, and references therein.

[9] A. Geiser, Ph.D. thesis, RWTH Aachen, 1992, Aachen report PITHA 92/31.

[10] P. Nason, S. Dawson, and R.K. Ellis, Nucl. Phys. **B303** (1988) 607;
P. Nason, S. Dawson, and R.K. Ellis, Nucl. Phys. **B327** (1989) 49.

[11] W. Beenakker et al., Phys. Rev. **D40** (1989) 54;
W. Beenakker et al., Nucl. Phys. **B351** (1991) 507.

[12] A.D. Martin, R.G. Roberts and W.J. Stirling, Phys. Rev. **D43** (1991) 3648.

[13] A.D. Martin, W.J. Stirling and R.G. Roberts, Phys. Rev. **D47** (1993) 867;
A.D. Martin, W.J. Stirling and R.G. Roberts, Phys. Lett. **B306** (1993) 145.

[14] ZEUS collaboration, M. Derrick et al., Phys. Lett. **B316** (1993) 207;
H1 collaboration, I. Abt et al., Nucl. Phys. **B407** (1993) 515.

[15] M. Diemoz, F. Ferroni, E. Longo and G. Martinelli, Z. Phys. **C39** (1988) 21.

[16] A.D. Martin, R.G. Roberts and W.J. Stirling, Phys. Rev. **D37** (1988) 1161.

[17] H. Plothow-Besch, *Parton density functions*, Proceedings of the 3rd Workshop on Detector and Event Simulation in High Energy Physics, Amsterdam, 8–12 April 1991;
H. Plothow-Besch, *PDFLIB: Structure function and α_s calculation user's manual, version 2.00*, and references therein, CERN program library entry W5051, 1991, unpublished.

[18] W.A. Bardeen, A.J. Buras, D.W. Duke and T. Muta, Phys. Rev. **D18** (1978) 3998.

[19] Particle Data Group, K. Hikasa et al., Phys. Rev. **D45** (1992) 1.

[20] CDF collaboration, F. Abe et al., Phys. Rev. Lett. **68** (1992) 1105.